



The discovery of novel sanjuanolide derivatives as chemotherapeutic agents targeting castration-resistant prostate cancer

Guangbao Wang^{a,1}, Xiaojing Chen^{a,1}, Nan Wang^{a,1}, Yunbei Xiao^{b,1}, Sheng Shu^a,
Ali Mohammed Mohammed Alsayed^a, Lu Liu^a, Yue Ma^a, Peng Liu^a, Qianwen Zhang^a,
Xiangjuan Chen^{c,*}, Zhiguo Liu^{a,*}, Xiaohui Zheng^{a,*}

^a Chemical Biology Research Center at School of Pharmaceutical Sciences, Wenzhou Medical University, 1210 University Town, Wenzhou, Zhejiang 325035, China

^b Department of Urology, The First Affiliated Hospital of Wenzhou Medical University, Wenzhou 325000, Zhejiang, China

^c Department of Obstetrics and Gynecology, Shenzhen University General Hospital, Shenzhen University, Shenzhen, Guangdong 518000, China

ARTICLE INFO

Keywords:

Sanjuanolide
Castration-resistant prostate cancer
Anticancer activity
DNA damage
DNA damage response

ABSTRACT

There remains a critical need for more effective therapies for the treatment of castration-resistant prostate cancer (CRPC), which is the leading cause of death in patients with prostate cancer. In this study, a series of sanjuanolide derivatives were designed, synthesized and evaluated as potential anti-CRPC agents. Most of the compounds had excellent selectivity for CRPC cells with IC_{50} values $< 20 \mu\text{M}$. Moreover, minimal side effects on human normal hepatic MIHA cells and normal prostatic stromal myofibroblast WPMY-1 cells were observed, with $IC_{50} > 100 \mu\text{M}$. The representative compound **S07** slowed down the proliferative rate of CRPC cells, promoted cell apoptosis and caused G2/M phase accumulation, as well as G1/G0 phase reduction. Further mechanistic studies showed that **S07** treatment triggered intense DNA damage and provoked strong DNA damage response in a dose-dependent manner. These findings suggested that sanjuanolide derivatives, especially **S07**, selectively induced CRPC cell death by triggering intense DNA damage and DNA damage response.

1. Introduction

Castration-resistant prostate cancer (CRPC) is defined by disease progression despite androgen-deprivation therapy (ADT) and is mainly developed from prostate cancer with ADT treatment [1]. It is the leading cause of death in prostate cancer patients [2–5]. At present, surgery, chemotherapy, radiotherapy and immunotherapy are the primary treatment options for CRPC [5–7]. Among them, chemotherapy is the first choice for oncologists against metastatic CRPC [8–10]. However, it has been reported that cancer cells can become drug resistant, which can limit the effectiveness of expensive agents used to treat cancer and/or lead to chemotherapy failure [4,5,11–13]. With these concerns, the design and discovery of more effective drug candidates that selectively target CRPC cells, with minimal side effects and low cost, could have

potential advantages as CRPC therapeutics.

Sanjuanolide (1, Fig. 1) is an isoprenylated chalcone first isolated from *Dalea frutescens* A. Gray (Leguminosae) in 2016. In *in vitro* studies, it exhibited promising anti-proliferative activity against PC3 and DU145 prostate cancer cells [14]. To further study the pharmacological action of sanjuanolide, we have recently completed the first total synthesis of (R)-, (S)- and (±)-sanjuanolide by a new and efficient synthetic strategy. Additional biological studies have shown that the (R)-sanjuanolide is important for anti-inflammatory activity [15]. Additionally, our previous studies indicated that chalcones, with an allyl or isoprenyl moiety at position 5 in the A ring, showed effective inhibitory activity against cancer and related diseases [16]. Thus, we proposed that replacement of the isoprenyl group with an allyl moiety in sanjuanolide may provide equivalent or better biological activity.

Abbreviations: CRPC, Castration-resistant prostate cancer; ADT, Androgen-deprivation therapy; MOM, Methoxymethyl; TBS, *t*-Butyldimethyl; DMF, Dimethyl Formamide; MTT, 3-(4,5-Dimethylthiazol-2-yl)-2,5-diphenyl tetrazolium bromide; PARP, Poly ADP-ribose polymerase; Bcl2, B-cell lymphoma-2; FCM, Flow cytometry; DSBs, DNA double-strand breaks; DDR, DNA damage response; IF, Immunofluorescence.

* Corresponding authors at: Department of Obstetrics and Gynecology, Shenzhen University General Hospital, Shenzhen University, Shenzhen, Guangdong 518000, China. (X. Chen). Chemical Biology Research Center at School of Pharmaceutical Sciences, Wenzhou Medical University. 1210 University Town, Wenzhou, Zhejiang 325035, China. (Z. Liu, X. Zheng).

E-mail addresses: 472346758@qq.com (X. Chen), lzgcnu@163.com (Z. Liu), zhengxh@wmu.edu.cn (X. Zheng).

¹ These authors contribute equally to this work.

<https://doi.org/10.1016/j.bioorg.2021.104880>

Received 5 October 2020; Received in revised form 26 March 2021; Accepted 26 March 2021

Available online 29 March 2021

0045-2068/© 2021 Elsevier Inc. All rights reserved.

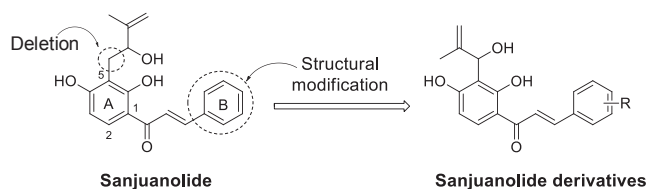


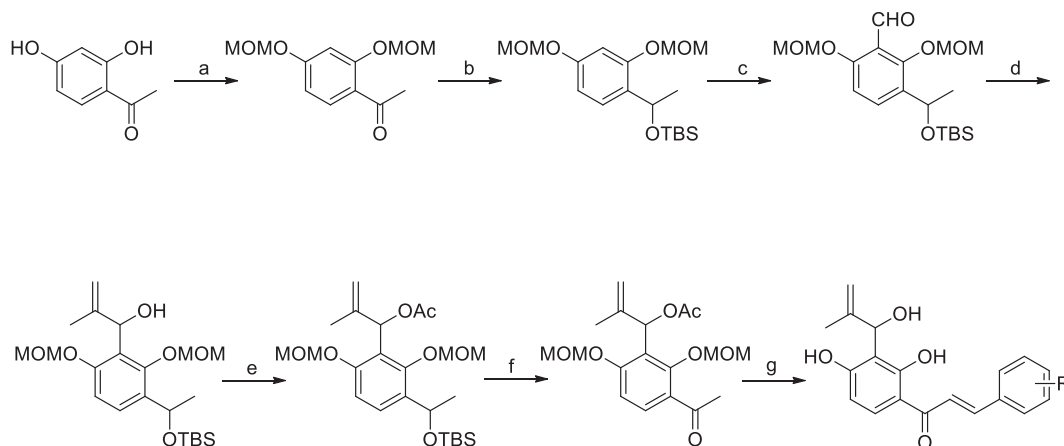
Fig. 1. Chemical structures of sanjuanolide and the structural design of new sanjuanolide derivatives.

Inspired by these results, we aimed to discover novel CRPC therapeutic agents by replacing the substituted 2-methyl-3-hydroxyisoprenyl group in sanjuanolide with a simple 2-methyl-3-hydroxyallyl group. Moreover, optimization of the phenyl substituents on the B ring may provide new lead compounds with enhanced CRPC activity. To our knowledge, these types of sanjuanolide derivatives have not yet been previously synthesized. Importantly, active derivative **S07** showed improved anti-tumor activities by triggering intense DNA damage and DNA damage response against castration-resistant prostate cancer (CRPC) *in vitro* and *in vivo*, suggesting the potential for sanjuanolide derivatives to be developed as new anti-cancer agents for the treatment of CRPC.

2. Results and discussion

2.1. Chemistry

The synthesis of sanjuanolide derivatives (**S01-S18**) was accomplished as portrayed in Scheme 1, and their structures are shown in Table 1. MOM protection of commercially available 2,4-dihydroxyacetophenone (**2**), followed by NaBH₄ reduction, provided 1-[2,4-bis(methoxymethoxy)phenyl]ethanol (**3**). The secondary alcohol **3** was protected by TBS to give (1-(2,4-bis(methoxymethoxy)phenyl)ethoxy)(*tert*-butyl)dimethylsilane (**4**). Treatment of **4** with *n*-BuLi and DMF afforded the aldehyde **5**, which was reacted efficiently with isopropenylmagnesium bromide to give the corresponding allylic alcohol **6** in good yield. Subsequently, acetylation of the alcoholic hydroxyl group with acetyl chloride yielded the corresponding 1-(3-(1-((*tert*-butyldimethylsilyl)oxy)ethyl)-2,6-bis(methoxymethoxy)phenyl)-2-methylallyl acetate (**7**), according to the procedure reported by Fang et al [15]. Furthermore, preparation of acetophenone **9** was achieved through the TBS-deprotection of **7** with TBAF, followed by oxidative workup of acetyl chloride **8** with Dess-Martin periodinane in EtOH. Finally, aldol condensation between the acetophenone **9** and various benzaldehydes



Scheme 1. General synthetic routes for **S01-S18**. Reagents and conditions: (a) i) NaH, MOMCl, THF, 0 °C, 4 h, ii) NaBH₄, EtOH, 0 °C, 3 h, 81%; (b) TBSCl, imidazole, CH₂Cl₂, rt, 6 h, 100%; (c) *n*-BuLi, DMF, THF, -78 °C to 0 °C, 3 h, 58%; (d) isopropenylmagnesium bromide, THF, 0 °C, 2 h, 63%; (e) DMAP, Et₃N, Ac₂O, CH₂Cl₂, 2 h, 88%; (f) TBAF, THF, rt, 5 h, 92%; (g) Dess-Martin periodinane, CH₂Cl₂, 4 h, 63%; (h) i) NaOH, EtOH, rt, overnight, ii) 4 M HCl, MeOH, 70 °C, 1.5 h, 35%–50%.

Table 1
Chemical structures and IC₅₀ (μM) values determined by the MTT assay.^a

Compound	R	IC ₅₀ (μM) PC3 ^b	DU145 ^b	MIHA ^b	WPMY-1 ^b
S01	–	21.04 ± 0.24	46.16 ± 1.16	>100	>100
S02	4'-Br	19.6 ± 0.39	58.05 ± 2.81	>100	>100
S03	4'-NO ₂	12.56 ± 0.02	12.04 ± 0.08	26.1 ± 0.10	32.81 ± 0.10
S04	2'-CF ₃	>100	>100	>100	>100
S05	3'-CF ₃	19.37 ± 0.51	37.02 ± 6.01	35.23 ± 4.27	37.8 ± 0.22
S06	4'-CF ₃	>100	40.78 ± 0.43	>100	>100
S07	4'- methylpiperazine	15.55 ± 0.51	6.77 ± 0.17	>100	>100
S08	4'- morpholine	29.80 ± 1.95	>100	>100	>100
S09	2'-OMe	26.47 ± 0.96	53.12 ± 0.35	63.17 ± 1.21	40.93 ± 1.05
S10	3'-OMe	26.46 ± 3.36	46.52 ± 0.55	83.11 ± 2.73	60.92 ± 4.31
S11	4'-OMe	50.01 ± 2.66	88.74 ± 4.36	68.26 ± 1.41	51.43 ± 1.20
S12	2',3'-OMe	28.07 ± 0.18	>100	59.71 ± 2.557	83.62 ± 1.63
S13	3',4'-OMe	87.94 ± 4.36	>100	>100	22.44 ± 0.57
S14	2',4'-OMe	>100	>100	>100	>100
S15	2',5'-Me	>100	>100	>100	>100
S16	3'-OMe, 4'-OH	>100	85.16 ± 4.80	>100	>100
S17	2',4',6'-OMe	10.93 ± 0.55	>100	>100	>100
S18	3',4',5'-OMe	18.43 ± 0.37	15.67 ± 0.45	29.55 ± 2.03	22.44 ± 0.57
Sanjuanolide		7.78 ± 0.26	20.3 ± 0.38	>100	>100
Cisplatin		6.21 ± 0.54	25.68 ± 1.79	36.62 ± 0.61	51.6 ± 1.19

^a IC₅₀ values were drug concentrations necessary for 50% inhibition of cell viability. Data are average ± standard deviations of at least three independent experiments. The drug treatment period was 48 h. ^b Human castration-resistant prostate cancer (CRPC) cells, PC3 and DU145; human normal hepatic cells (MIHA) and human normal prostatic stromal myofibroblast cells (WPMY-1).

in ethanolic KOH solution resulted in protected target molecules. The target molecules were deprotected with concentrated HCl in methanol, generating target compounds **S01**–**S18** over two steps. Both analytical and spectral data of all synthesized compounds are in full agreement with the proposed structures.

2.2. The cytotoxicity and antiproliferative activities of synthetic compounds toward castration-resistant prostate cancer

The anticancer activity of the synthesized compounds was evaluated for potential anti-castration-resistant prostate cancer (CRPC) activity using MTT assay, while the well-known anticancer drug cisplatin and sanjuanolid were used as the positive controls. Human CRPC cells, PC3 and DU145, were cultured in the presence or absence of test compounds for 48 h, and the cell viabilities were determined. The results are summarized in Table 1. The initial screening showed that compared to human normal hepatic cells (MIHA) and human normal prostatic stromal myofibroblast cells (WPMY-1), a majority of compounds preferred to exhibit higher cytotoxicity to both CRPC PC3 and DU145 cells. This suggests that compounds **S01**–**S18** could potentially be developed as selective antitumor agents against CRPC. Among the 15 tested compounds studied, compound **S07**, with 4-methylpiperazine at the R position, proved to be the most active against PC3 and DU145 cells, with IC_{50} values of 15.55 μ M and 6.77 μ M, respectively. In addition, compound **S07**, possessed comparable anticancer activity to cisplatin, but **S07** had fewer side effects. Thus, it was selected as a candidate in this study.

To investigate the influence of the B ring substituents on the anticancer activity, we introduced various electron-withdrawing groups, such as bromine, nitro group and trifluoromethyl groups at the phenyl ring in compound **S01**, resulting in compounds **S02**–**S06**. Compounds **S02**, **S03** and **S05** demonstrated equal or greater potency against PC3

and DU145 cells, relative to compounds **S01**. However, compound **S04**, with a trifluoromethyl moiety at the *ortho*-position of the phenyl ring, resulted in a dramatic loss of anti-proliferative activity, indicating that the introduction of an electron-withdrawing group at the *ortho*-position is not beneficial to the activity. Interestingly, compound **S07**, which has a 4'-methylpiperazine at the *para*-position of the phenyl ring, displayed the greatest activity against PC3 and DU145 cells. Replacement of 4-methylpiperazine of **S07** with a morphine motif (compound **S08**) resulted in a substantial reduction or loss of anti-proliferative effects.

The introduction of 2'-methoxy (compound **S09**) or 3'-methoxy (compound **S10**) substitution showed an almost equivalent activity in comparison with the compounds **S01** on PC3 and DU145 cells. However, the introduction of methoxy (compound **S11**) to the C-4' position, as oppose to phenyl ring, resulted in a substantial loss of anti-proliferative effects. Finally, incorporation of different disubstituted or trisubstituted electron-donating groups onto the phenyl ring provided compounds **S12**–**S18**, and these compounds displayed varying degrees of inhibition toward PC3 cells. However, almost no activity toward DU145 cells was observed, except for compound **S18** with an IC_{50} value of 15.67 μ M. Taken together, the structure–activity relationships in this series are complex, but the data provide valuable information for the design of novel anti-cancer agents.

2.3. Active compound S07 inhibits cell proliferation and disrupts tubulin polymerization

In order to further explore the antiproliferative activity of active compound **S07** in CRPC cells, the long-term proliferation assay was carried out under the $0.5IC_{50}$ and IC_{50} values at the indicated concentrations 4.0 μ M, 8.0 μ M or 16.0 μ M. The results clearly showed that even in a relatively low dose, **S07** could significantly slow down the

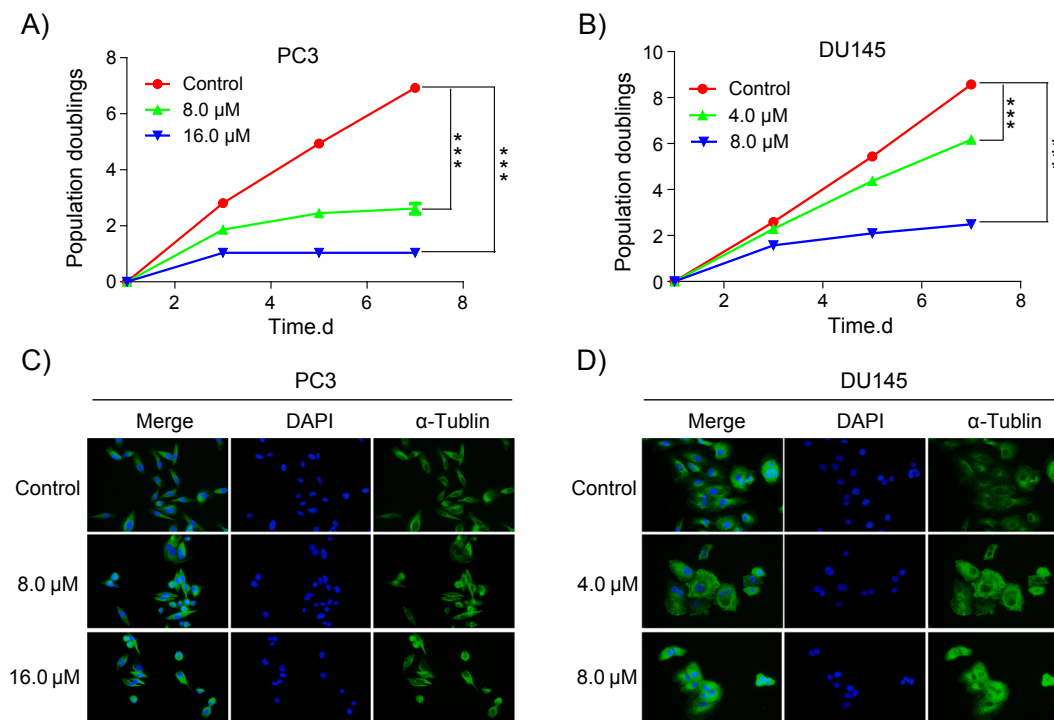


Fig. 2. **S07** inhibits the proliferation and disrupts tubulin polymerization of castration-resistant prostate cancer (CRPC) cells. The proliferation curves of PC3 (A) and DU145 (B) in the control and **S07**-treated cells at the indicated concentrations of $0.5IC_{50}$ and IC_{50} concentrations of **S07** upon PC3 (8.0 μ M and 16.0 μ M) and DU145 (4.0 μ M and 8.0 μ M), respectively. Values are the average \pm SD of three independent experiments. p values were calculated using Two-way ANOVA (* p < 0.05, ** p < 0.01, *** p < 0.001). Immunofluorescence assay analysis of the effect of **S07** on the organizations of cellular microtubule network. PC3 (C) and DU145 (D) cells were treated with $0.5IC_{50}$ and IC_{50} concentrations of **S07** upon PC3 (8.0 μ M and 16.0 μ M) and DU145 (4.0 μ M and 8.0 μ M), respectively. Then, microtubules were stained with anti- α -tubulin-FITC antibody (green), and nucleuses were stained with DAPI (blue). Images were performed by using Nikon microscope (Nikon, Japan). (For interpretation of the references to colour in this figure legend, the reader is referred to the web version of this article.)

proliferation rate of CRPC PC3 and DU145 cells (Fig. 2A and 2B). Considering the results from MTT assay and long-term proliferation assay together, the $0.5IC_{50}$ and IC_{50} concentrations of **S07** were chosen in the following assay. Furthermore, we observed that compared with untreated group, **S07** treatment would disrupt the tubulin polymerization and organization of CRPC PC3 and DU145 cells (Fig. 2C and 2D) in a concentration-dependent manner. Since the tubulin polymerization and functional organization played a key role of cell mitosis [17], **S07** might finally lead to cell cycle arrest due to the inhibition of tubulin polymerization.

2.4. Active compound **S07** arrests cell cycle of PC3 and DU145 cells in G2/M phase

In order to explore the *in vivo* evidence that active compound **S07** slowed down the proliferation rate of CRPC cells by cell cycle arrest. The cell cycle distribution of CRPC cells PC3 and DU145 treated and/or untreated with active compound **S07** for 48 h was analyzed by flow cytometry assay. As shown in Fig. 3, **S07** arrested both PC3 and DU145 cells at the G2/M phase in a dose-dependent manner. It is worth noting

that **S07** treatment increased the percentage of G2/M phase and S phase cells while reducing the percentage of cells in the G0/G1 phase relative to the control. Since cells transverse the cell cycle in several well-controlled phases: cells commit to enter the cell cycle in G1/G0 phase and prepare to duplicate their DNA in S phase, then chromatids and daughter cells separate in M phase [18]. Furthermore, it has been reported that G1/G0 phase arrest might enhance proliferation, and G2/M phase arrest might result in cell apoptosis [19]. **S07** arrested CRPC cells at the G2/M and S phases and reduced the G0/G1 phase, demonstrating that the slower CRPC cell proliferation rate in **S07**-treated cells might also induce CRPC cell apoptosis.

2.5. Active compound **S07** induces cell apoptosis by regulating the expression of apoptosis-related protein

Apoptosis is the common anticancer mechanism of natural products, and the cell cycle arrest data indicated that **S07** would induce cell apoptosis. Therefore, the well-known apoptosis-related proteins, cleaved-PARP [20], caspase-3, cleaved-caspase-3 [21] and Bcl2, which are widely regarded as markers of apoptosis, were chosen in the western

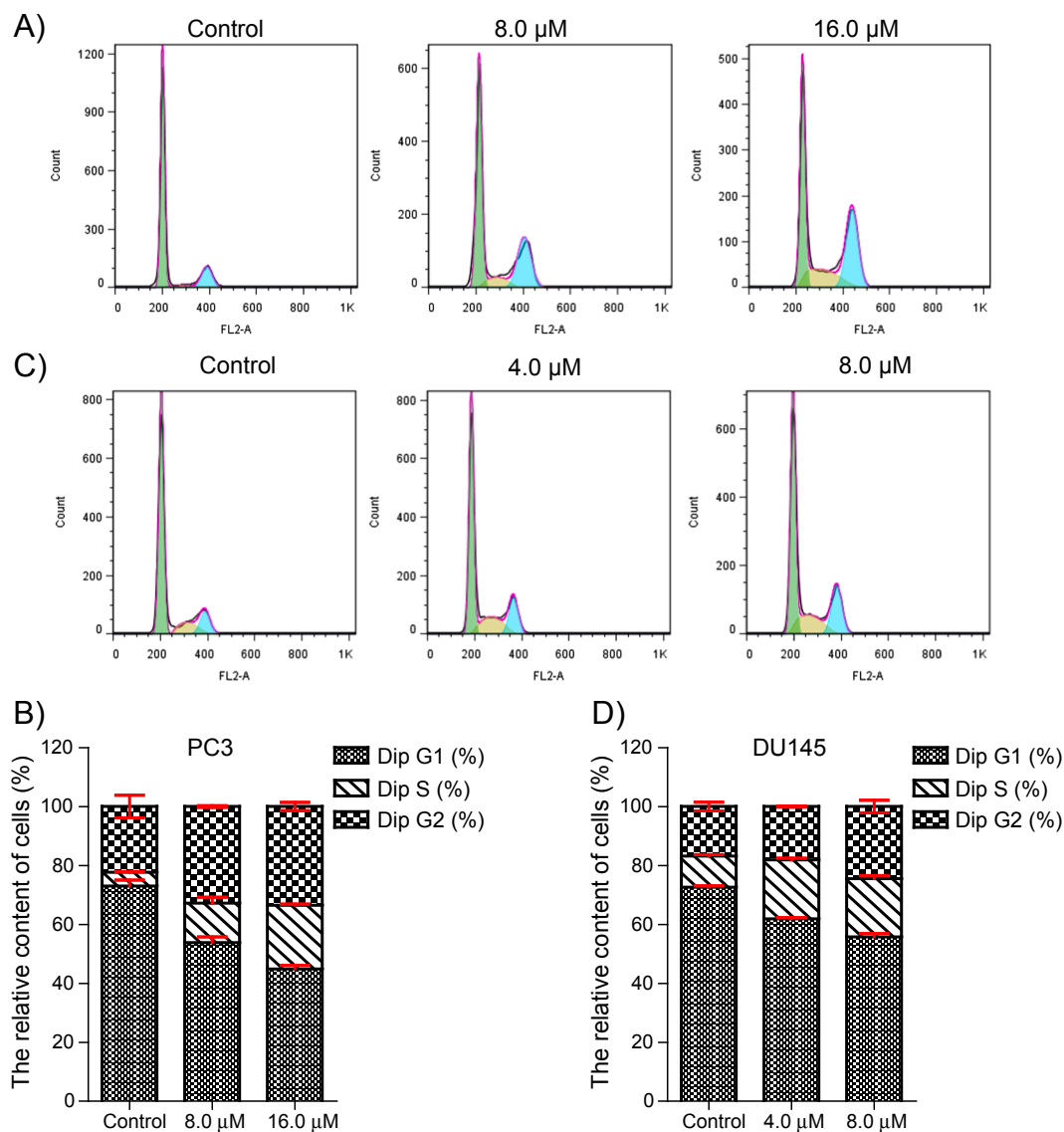


Fig. 3. G2/M phase arrest in **S07**-treated castration-resistant prostate cancer (CRPC) cells. $0.5IC_{50}$ and IC_{50} concentrations of **S07**-treated PC3 (8.0 μM and 16.0 μM) and DU145 (4.0 μM and 8.0 μM), or untreated cells (Control) were subjected to cell cycle FACS analysis. The representative images of **S07**-treated PC3 (A) and DU145 (C) cells. **B** and **D**, Quantification of A and C. Values are average \pm SD of three independent experiments.

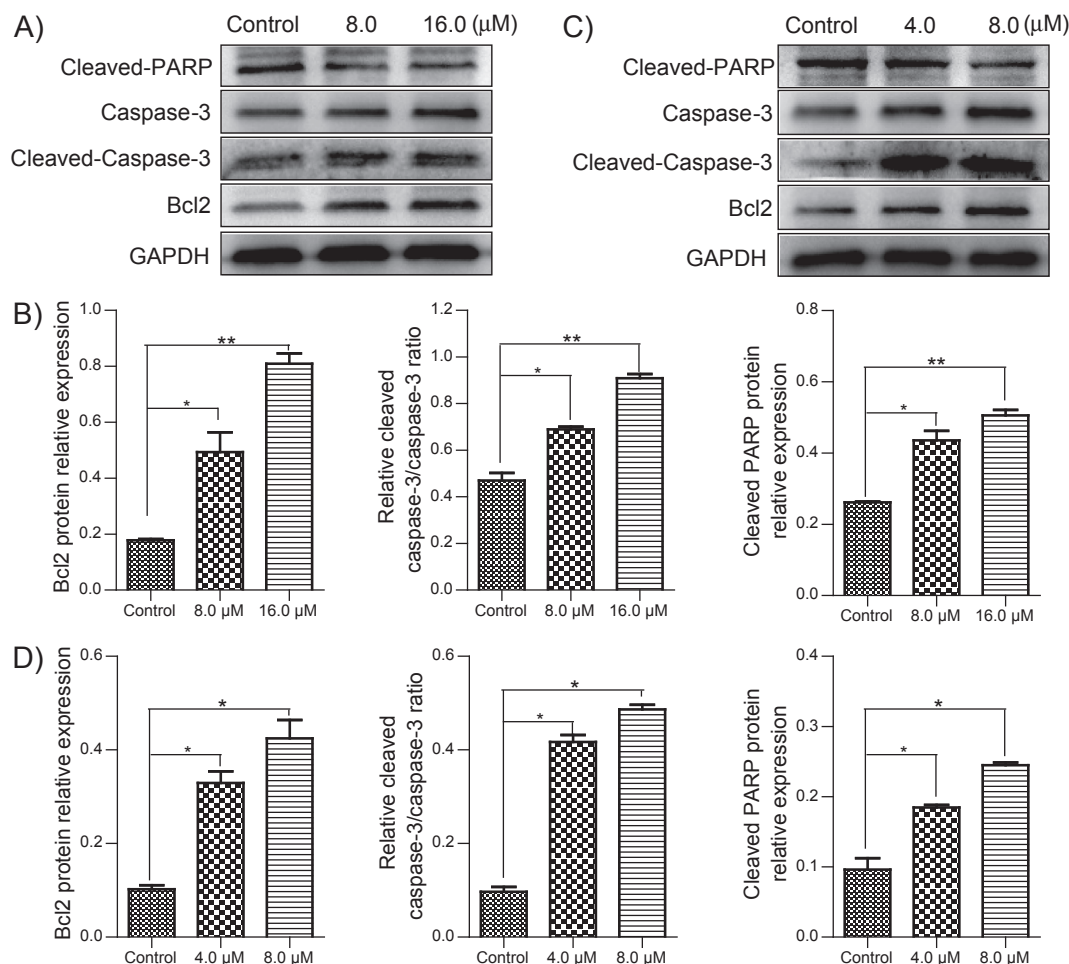


Fig. 4. S07 regulates the expression of apoptosis-related proteins cleaved-PARP, caspase-3, cleaved-caspase-3 and Bcl2 in castration-resistant prostate cancer (CRPC) cells. Western blot determination of the abundance of cleaved-PARP, caspase-3, cleaved-caspase-3 and Bcl2 in the control and S07-treated PC3 (A) and DU145 (C) cells. Cells were treated with 0.5IC₅₀ and IC₅₀ concentrations of S07-treated PC3 (8.0 μM and 16.0 μM) and DU145 (4.0 μM and 8.0 μM) for 48 h and subjected to western blot using antibodies against cleaved-PARP, caspase-3, cleaved-caspase-3 and Bcl2. GAPDH was used as a loading control. B and D, Quantification of A and C. Values are average ± SD of three independent experiments. Unpaired Student's two-tailed *t* test was used to determine the statistical significance (**p* < 0.05, ***p* < 0.01).

blot assay. The results show that S07 decreased the expression of cleavage-PARP and increased the expression of caspase-3 and Bcl2 proteins in a dose-dependent manner (Fig. 4). The results further indicate that S07 induces cell apoptosis by regulating the expression of apoptosis-related proteins, PARP, caspase-3 and Bcl2.

To test this, flow cytometry (FCM) assay was performed to analyze the cell apoptosis in control and S07 treated CRPC cells. Consequently, S07 induced CRPC cells apoptosis at a dose- and time-dependent manner, especially in time-dependent manner (Fig. 5 and Figure S1). To exclude the possibility that S07 might induce CRPC cell senescence, a beta-galactosidase (SA-β gal) staining assay was performed in the present or absent of S07 treated CRPC cells. We observed that there is no significant difference in the percentage of senescent cells between untreated group and S07-treated group (Figure S2), demonstrating that S07 did not induce cell senescence. Taken together, these results indicate that S07 could induce apoptosis in CRPC cells, presumably as a result of its effects on the expression of apoptosis-related protein PARP, caspase-3 and Bcl2. This is consistent with other reports showing that the cleaved-PARP, caspase-3 and Bcl2 levels correlate with cell cycle arrest and apoptosis [20,21].

2.6. Active compound S07 treatment triggered intense DNA damage

Chemotherapy agents, such as some natural products, are used to kill

cancer cells by introducing mass DNA damage [22]. This is based on the widely accepted concept that nonproliferating cells are more resistant to DNA damage and/or DNA damage response than proliferating cells [23]. To investigate DNA damage in S07-treated human CRPC cells, PC3 and DU145 cells were exposed to 4.0, 8.0 or 16.0 μM of S07 for 48 h, and the level of DNA damage was assessed by comet assay. As expected, S07 induced a significant amount of DNA damage in PC3 and DU145 cells, leading to DNA fragments that leave the genome and form "tails" during the neutral and alkaline comet assay (Fig. 6A and 6C, Figure S3A and S3C). A percentage of tail DNA was used to indicate the abundance of fragments induced by DNA lesions. The results show that the level of DNA damage in S07-treated CRPC cells significantly increased in a concentration-dependent manner (Fig. 6B and Figure S3B). Accordingly, >20% of cells displayed higher DSB levels than the control (5% tail DNA signal) (Fig. 6D and Figure S3D). Collectively, these results demonstrate that active compound S07 achieved excellent anticancer activity by triggering intense DNA damage.

2.7. Active compound S07 treatment provoked strong DNA damage response

The ability to repair DNA lesion is critical for cell viability [24,25], and previous reports indicated that cancer cells are endowed with that same innate, or even stronger, DNA repair capacity as normal cells [24].

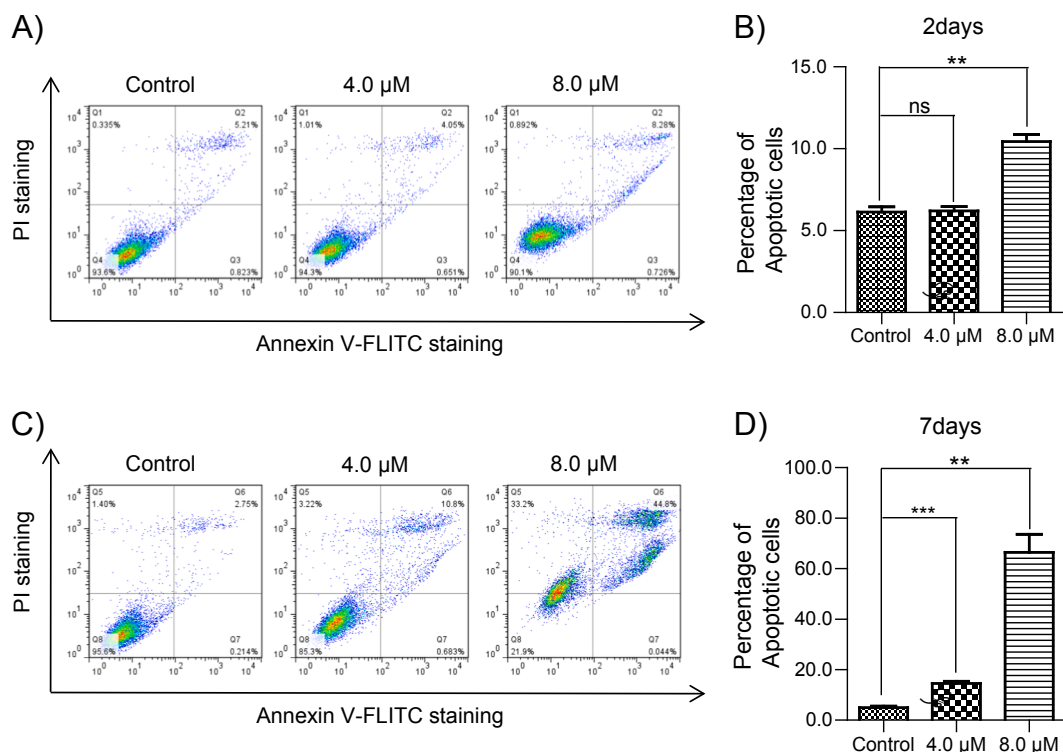


Fig. 5. S07 treatment induces apoptosis of castration-resistant prostate cancer (CRPC) cells. FACS analysis was performed to detect the apoptotic DU145 cells treated with 0.5 IC_{50} and IC_{50} concentrations of S07-treated PC3 (8.0 μ M and 16.0 μ M) or DU145 (4.0 μ M and 8.0 μ M), for 2 days (A) and/or 7 days (C). B and D, Quantification of A and C. Values are average \pm SD of three independent experiments. Unpaired Student's two-tailed t test was used to determine the statistical significance (* p < 0.05, ** p < 0.01, *** p < 0.001).

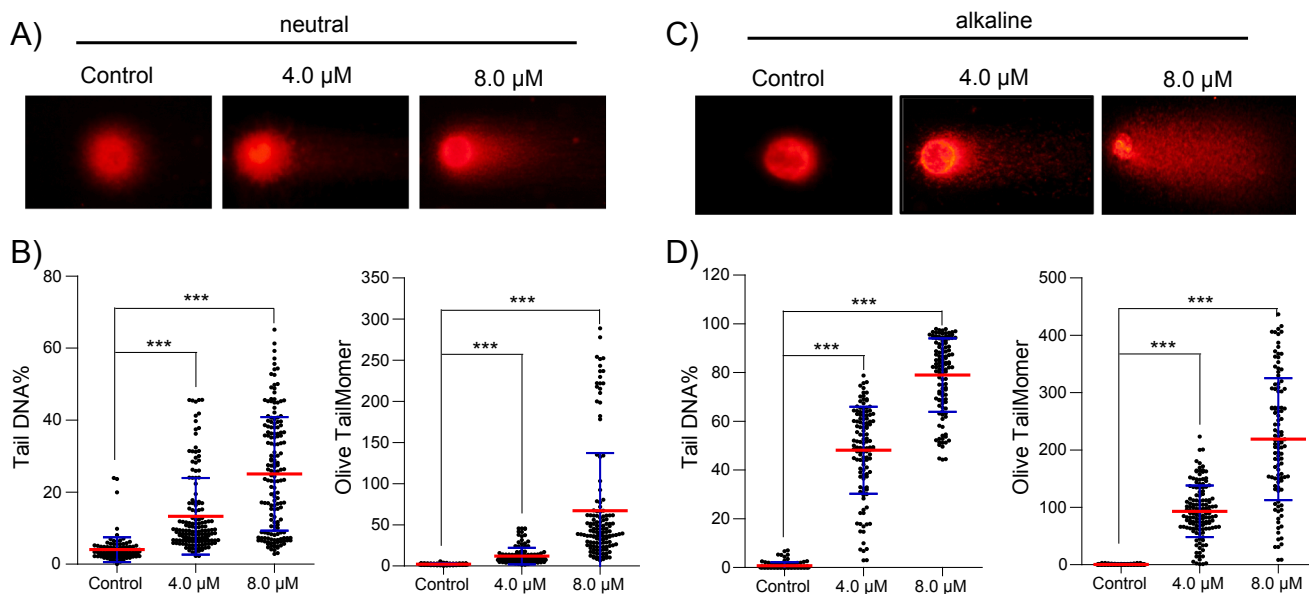


Fig. 6. S07 treatment triggers intense DNA damage in castration-resistant prostate cancer (CRPC) DU145 cells in a concentration-dependent manner. A and C, Representative images of comet assay in neutral and alkaline of 0.5 IC_{50} and IC_{50} concentrations of S07-treated DU145 (4.0 μ M and 8.0 μ M), respectively. B and D, The percentages of DNA in the tail for S07-treated DU145 and the percentage of S07-treated DU145 with over 10% tail DNA. Cells were treated with indicated concentration of S07 for 48 h, and \geq 500 cells were examined in each group. Values are average \pm SD of three independent experiments. Unpaired Student's two-tailed t test was used to determine the statistical significance (*** p < 0.001).

Persistent DNA double-strand breaks (DSBs) induce a potent DNA damage response (DDR), leading to cell cycle arrest, cell senescence or apoptosis that ultimately results in lethality at the cellular level [26]. To explore the fate of S07-induced DNA lesions, immunofluorescence (IF) assay was performed, using antibody to 53BP1 (a widely used marker for

DSBs) [27]. In Fig. 7, the number of 53BP1 foci per nucleus was calculated in both the control and S07-treated PC3 and/or DU145 cells. As expected, the number of 53BP1 foci in PC3 cells increased to an average of \sim 13 foci per nucleus 48 h after 10 μ M S07 treatment, and the number of 53BP1 foci per cell was found to be dose-dependent. Interestingly, the

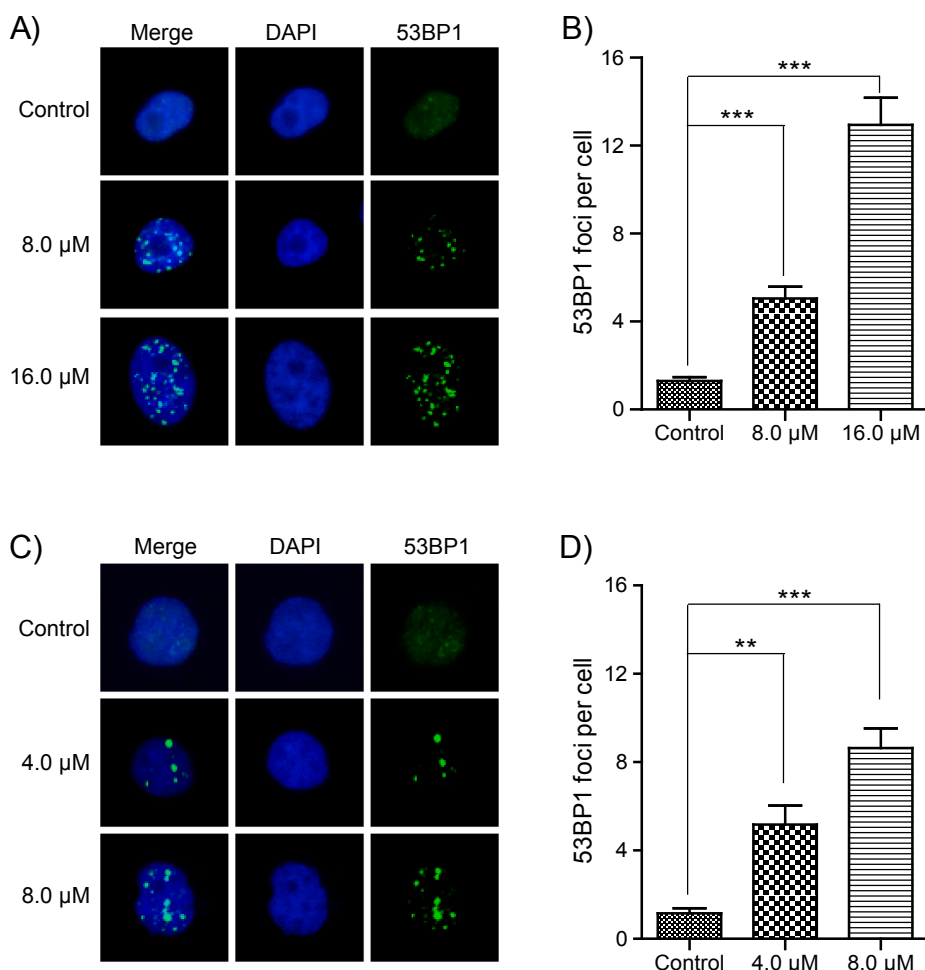


Fig. 7. S07 treatment provokes intense DNA damage response in castration-resistant prostate cancer (CRPC) cells in a concentration-dependent manner. A and C, Representative images of 53BP1 foci in PC3 and DU145 cells at the 0.5 $I_{C_{50}}$ and $I_{C_{50}}$ concentrations of S07-treated PC3 (8.0 μM and 16.0 μM) and DU145 (4.0 μM and 8.0 μM), respectively. B and D, Quantifying 53BP1 foci per cell of A and C, respectively. Cells were treated with S07 for 48 h, and ≥ 200 cells were examined in each group. Values are average \pm SD of three independent experiments. Unpaired Student's two-tailed t test was used to determine the statistical significance (** $p < 0.01$, *** $p < 0.001$).

relative intensity of 53BP1 foci also increased accordingly (Fig. 7A). We obtained similar results when DU145 cells were exposed to various concentrations of S07 (Fig. 7B). The results are consistent with the results from the western blot assay, showing S07 treatment significantly increased the expression of γ -H2AX and Rad 51 (Fig. 8) in a dose-dependent manner. These results, combined the data from comet assay, further supported the conclusion that S07 induced the death of CRPC cells by triggering strong DNA damage and DNA damage response.

2.8. Molecular docking

Binding of small organic ligands to DNA is among the widely used strategies for the development of novel antitumor therapeutics [28,29]. To investigate the structural mechanism underlying S07 binding to DNA, we docked the S07 molecule into the crystal structure of DNA by using the software Auto Dock 4.0. As shown in Fig. 9, the entire S07 molecule lodges inside the major groove of double-stranded DNA. From the in-silico modeling analysis, several hydrogen bonds were predicted between compound S07 and the surrounding nucleotides in the drug binding pocket. DA-18 (adenine) was involved in two hydrogen bonding interactions by one of the interacting with the carbonyl oxygen atom of α , β -unsaturated carbonyl groups of S07, and the other amino hydrogen atom interacting with one of the phenolic group in S07. In addition, the carbonyl oxygen atom in DT-7 (thymine) also interacted, by hydrogen bonding, with the secondary alcohol and the phenolic group of S07, respectively. Similarly, the hydrogen atom in the N1 atom of the imidazole in DA-6 (adenine) was engaged in a hydrogen bond with the phenolic group of S07. Moreover, The 4'-methylpiperazine side chain of

S07 was exposed to water outside of DNA, as well mainly stabilized in a large hydrophobic cavity formed on the basis of a number hydrophobic nucleotides, including DC-15 (cytosine), DG-16 (guanine) and DA-17 (adenine), explaining why even as light change could not be tolerated at this position.

3. Conclusion

In conclusion, a series of novel sanjuanolid derivatives were designed and synthesized. The evaluation of their inhibitor activities against PC3 and DU145 cell lines showed the majority of synthetic compounds exhibited higher cytotoxicity to both PC3 and DU145 cells, compared to human normal MIHA and WPMY-1 cells. In general, derivative S07 showed the best anticancer activity on PC3 cells, with comparable cytotoxicity to the lead compounds sanjuanolid and cisplatin. Further mechanism studies showed that S07 inhibited cell viability, arrested the cell cycle and induced cell death of castration-resistant prostate cancer (CRPC) cells by triggering intense DNA damage and provoking stronger DNA damage response. These results reveal the potential of sanjuanolid derivatives as a novel chemotherapeutic agent for targeting CRPC cells.

4. Materials and methods

4.1. Chemistry

4.1.1. General

All reagents and solvents were purchased from Alfa Aesar or Sigma

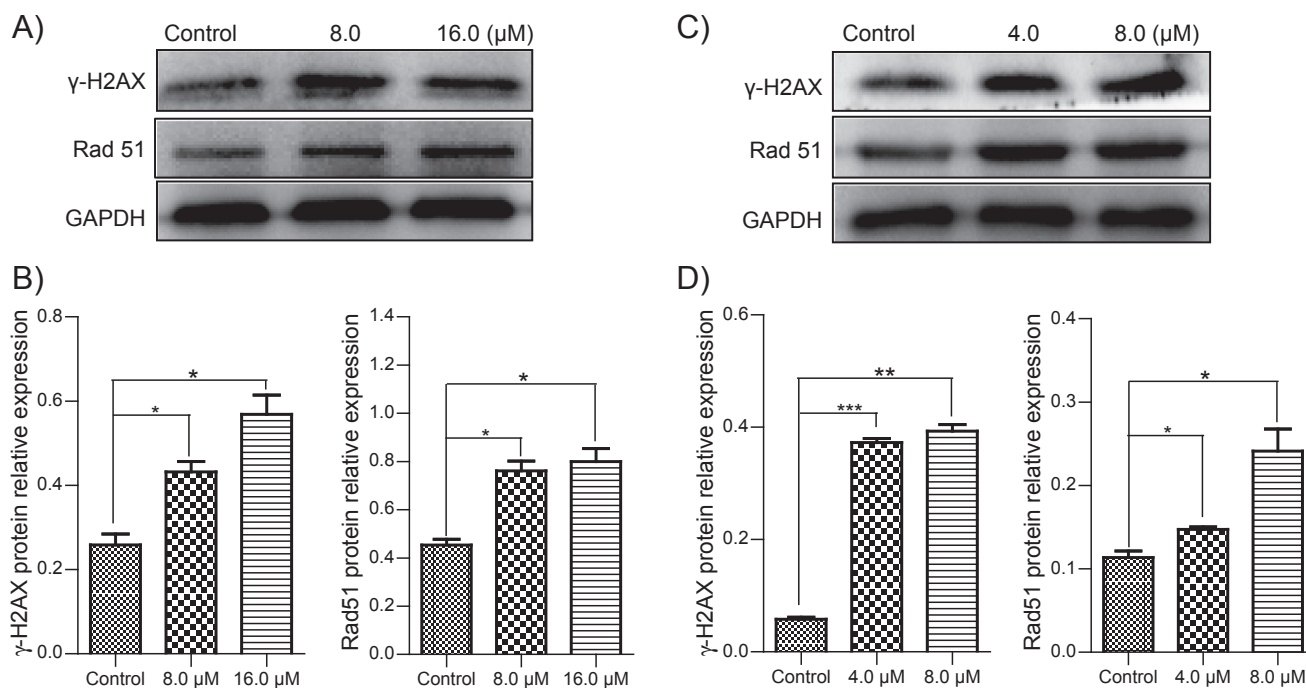


Fig. 8. S07 regulates the expression of DNA damage response-related protein γ -H2AX and Rad51 in castration-resistant prostate cancer (CRPC) cells. Western blot determination of the abundance of γ -H2AX and Rad51 in the control and S07-treated PC3 (A) and DU145 (C) cells. Cells were treated with $0.5IC_{50}$ and IC_{50} concentrations of S07 (PC3, 8.0 μ M and 16.0 μ M; DU145, 4.0 μ M and 8.0 μ M), for 48 h and subjected to western blot analysis using antibodies against γ -H2AX and Rad51. GAPDH was used as a loading control. B and D, Quantification of A and C. Values represent the average \pm SD of three independent experiments. Unpaired Student's two-tailed *t* test was used to determine the statistical significance (**p* < 0.05, ***p* < 0.01, ****p* < 0.001).

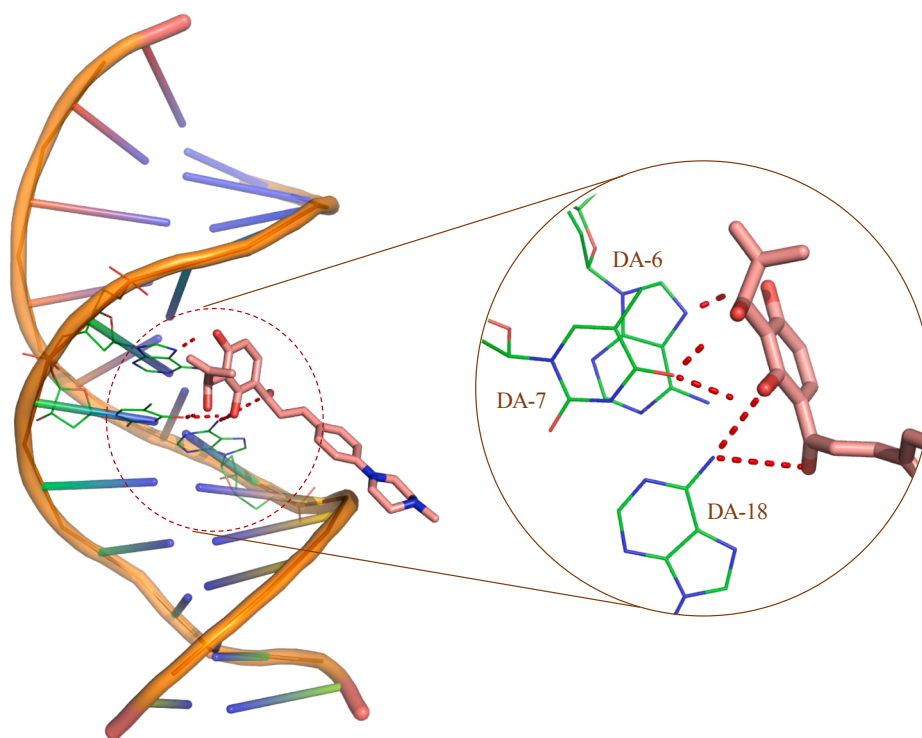


Fig. 9. The binding modes of S07 with the major groove of double-stranded DNA.

Aldrich and were used as received, unless noted otherwise. Thin layer chromatography was carried out using Kiesel-gel 60 F₂₅₄ glass-backed plates. Flash column chromatography was performed with silica gel 60 as the stationary phase. Melting points were determined on a Fisher-Johns melting apparatus and were uncorrected. Nuclear magnetic

resonance (NMR) spectra were recorded on a Bruker Avance DRX 500 instrument (¹H, 500 MHz, ¹³C, 126 MHz). The chemical shifts are expressed in parts per million relative to internal TMS, and coupling constants (*J*) are in Hz. Analytical liquid chromatography/mass spectrometry (LC/MS) was recorded on a Bruker Esquire 3000t Spectrometer.

4.1.2. Synthesis of 1-[2,4-bis(methoxymethoxy)phenyl]ethanol (3)

To a solution of 1-(2,4-dihydroxyphenyl)ethanone (1) (12.0 g, 78.9 mmol) in anhydrous THF (100 mL) was added sodium hydride in an ice-bath. After 30 min, the mixture was added chloromethyl methyl ether (19.1 g, 236.6 mmol) slowly. After stirring for 4 h at room temperature, the resulting mixture was poured into water (100 mL), extracted with EtOAc (3 × 50 mL). The combined organic layers were washed with water (100 mL), brine (100 mL), dried over anhydrous MgSO₄, filtered, and concentrated *in vacuo*.

The crude liquid (10.5 g, 43.7 mmol) was dissolved in EtOH (50 mL) at ice-bath temperature, followed by sodium borohydride (4.96 g, 43.7 mmol) and the mixture was then allowed to warm up to room temperature and stirring was continued for 3 h. The resulting mixture was quenched with saturated aqueous NH₄Cl (50 mL), and extracted with EtOAc (3 × 50 mL). The combined organic layers were washed with water (100 mL), brine (100 mL), dried over anhydrous MgSO₄, filtered, and concentrated *in vacuo*. The residue was purified by chromatography on silica gel to give compound 3 as a colorless oil (9.80 g, 81%). ¹H NMR (500 MHz, CDCl₃) δ (ppm): 7.28 (d, *J* = 10.0 Hz, 1H), 6.79 (s, 1H), 6.71 (d, *J* = 10.0 Hz, 1H), 5.21 (d, *J* = 5.0 Hz, 2H), 5.15 (s, 1H), 5.11 (d, *J* = 5.0 Hz, 2H), 5.09–5.08 (m, 1H), 3.49 (s, 3H), 3.47 (s, 3H), 1.19 (d, *J* = 5.0 Hz, 3H). ESI-MS *m/z*: 265.1 (M + Na)⁺.

4.1.3. Synthesis of 1-[2,4-bis(methoxymethoxy)phenyl]ethoxy}(*tert*-butyl)dimethylsilane (4)

To a solution of 1-[2,4-bis(methoxymethoxy)phenyl]ethanol (3) (9.70 g, 40.0 mmol) in anhydrous CH₂Cl₂ (20 mL) was added imidazole (8.18 g, 120.1 mmol) at room temperature followed by *tert*-butyldimethylsilyl chloride (TBSCl) (15.1 g, 100.1 mmol) and the mixture was stirred at this temperature for 6 h. The reaction mixture was quenched with saturated aqueous NH₄Cl (20 mL) and extracted with EtOAc (3 × 20 mL). The combined organic layers were washed with water (50 mL), brine (50 mL), dried over anhydrous MgSO₄, filtered, and concentrated *in vacuo*. The residue was purified by chromatography on silica gel provided compound 4 as a colorless oil (11.5 g, 100%). ¹H NMR (500 MHz, CDCl₃) δ (ppm): 7.42 (d, *J* = 10.0 Hz, 1H), 6.74 (s, 1H), 6.70 (d, *J* = 10.0 Hz, 1H), 5.18 (s, 2H), 5.17–5.167 (m, 1H), 5.15 (s, 1H), 3.49 (s, 3H), 3.48 (s, 3H), 1.35 (d, *J* = 5.0 Hz, 3H), 0.91 (s, 9H), 0.05 (s, 3H), –0.02 (s, 3H). ESI-MS *m/z*: 379.2 (M + Na)⁺.

4.1.4. Synthesis of 3-{1-[(*tert*-butyldimethylsilyloxy)ethyl]-2,6-bis(methoxymethoxy) benzaldehyde (5)

A 2.5 M solution of *n*-BuLi in THF (9.4 mL, 22.8 mmol) was added dropwise to a solution of 1-[2,4-bis(methoxymethoxy)phenyl]ethoxy}(*tert*-butyl)dimethylsilane (4) (5.80 g, 16.3 mmol) in anhydrous THF (30 mL) at –78 °C under a nitrogen atmosphere. After 1 h, dry DMF (4.0 mL, 26.0 mmol) was added dropwise. The reaction solution was then allowed to warm up to room temperature and stirring was continued for 2 h. The resulting solution was quenched with saturated aqueous NH₄Cl (20 mL) and extracted with EtOAc (3 × 20 mL). The combined organic layers were washed with water (100 mL), brine (100 mL), dried over anhydrous MgSO₄, filtered, and concentrated *in vacuo*. The residue was purified by chromatography on silica gel gave compound 5 as a yellow oil (3.60 g, 58.1%). ¹H NMR (500 MHz, CDCl₃) δ (ppm): 10.46 (s, 1H), 7.73 (d, *J* = 10.0 Hz, 1H), 7.01 (d, *J* = 10.0 Hz, 1H), 5.28–5.25 (m, 3H), 5.11 (d, *J* = 5.0 Hz, 1H), 5.00 (d, *J* = 5.0 Hz, 1H), 3.58 (s, 3H), 3.52 (s, 3H), 1.37 (d, *J* = 5.0 Hz, 3H), 0.90 (s, 9H), 0.06 (s, 3H), –0.03 (s, 3H). ESI-MS *m/z*: 407.2 (M + Na)⁺.

4.1.5. Synthesis of 1-{3-[1-[(*tert*-butyldimethylsilyloxy)ethyl]-2,6-bis(methoxymethoxy)phenyl]-2-methylprop-2-en-1-ol (6)

To a stirred solution of 3-{1-[(*tert*-butyldimethylsilyloxy)ethyl]-2,6-bis(methoxymethoxy) benzaldehyde (5) (2.30 g, 5.90 mmol) in anhydrous THF (20 mL) was added a 0.5 M solution of isopropenyl magnesium bromide in THF (13.0 mL, 8.9 mmol) slowly at –30 °C under a nitrogen atmosphere. The reaction solution was then allowed to warm up

to room temperature and stirring was continued for 2 h. The resulting solution was poured into water (20 mL) and extracted with EtOAc (3 × 20 mL). The combined organic layers were washed with water (50 mL), brine (50 mL), dried over anhydrous MgSO₄, filtered, and concentrated *in vacuo*. The residue was purified by chromatography on silica gel gave compound 6 as a yellow oil (1.46 g, 63%). ¹H NMR (500 MHz, CDCl₃) δ (ppm): 7.40 (d, *J* = 10.0 Hz, 1H), 6.93 (d, *J* = 10.0 Hz, 1H), 5.42 (s, 1H), 5.17–5.13 (m, 3H), 4.99–4.95 (m, 1H), 4.90–4.87 (m, 3H), 3.57 (s, 3H), 3.44 (s, 3H), 1.69 (s, 3H), 1.36 (d, *J* = 10.0 Hz, 3H), 0.85 (m, 9H), 0.04 (s, 3H), –0.04 (s, 3H). ESI-MS *m/z*: 450 (M + Na)⁺.

4.1.6. Synthesis of 1-{3-[1-[(*tert*-butyldimethylsilyloxy)ethyl]-2,6-bis(methoxymethoxy) phenyl]-2-methylallyl acetate (7)

A solution of 1-{3-[1-[(*tert*-butyldimethylsilyloxy)ethyl]-2,6-bis(methoxymethoxy)phenyl]-2-methylprop-2-en-1-ol (6) (1.41 g, 3.3 mmol) in dry CH₂Cl₂ (20 mL) was added Et₃N (1.5 mL, 9.9 mmol) portionwise, followed by acetic anhydride (0.72 mL, 6.6 mmol) and 4-dimethylaminopyridine (DMAP) (38 mg, 0.31 mmol) at room temperature. After 2 h, the reaction mixture was quenched with saturated aqueous NH₄Cl (20 mL) and extracted with EtOAc (3 × 20 mL). The combined organic layers were washed with a solution of aqueous citric acid (50 mL), brine (50 mL), dried over anhydrous MgSO₄, filtered, and concentrated *in vacuo*. The residue was purified by chromatography on silica gel gave compound 7 as a yellow oil (1.10 g, 88%). ¹H NMR (500 MHz, CDCl₃) δ (ppm): 7.44 (d, *J* = 10.0 Hz, 1H), 6.90 (d, *J* = 10.0 Hz, 1H), 6.76 (s, 1H), 5.24 (d, *J* = 5.0 Hz, 1H), 5.12–5.10 (m, 2H), 4.98 (d, *J* = 5.0 Hz, 1H), 4.93–4.86 (m, 2H), 4.78 (s, 1H), 3.55 (s, 3H), 3.44 (s, 3H), 2.07 (s, 3H), 1.61 (s, 3H), 1.35–1.33 (m, 3H), 0.84 (s, 9H), –0.01 (s, 3H), –0.10 (s, 3H). ESI-MS *m/z*: 491.3 (M + Na)⁺.

4.1.7. Synthesis of 1-[3-(1-hydroxyethyl)-2,6-bis(methoxymethoxy) phenyl]-2-methylallyl acetate (8)

A solution of 1-{3-[1-[(*tert*-butyldimethylsilyloxy)ethyl]-2,6-bis(methoxymethoxy) phenyl]-2-methylallyl acetate (7) (1.0 g, 2.13 mmol) in anhydrous THF (15 mL) was treated with *tetra-n*-butylammonium fluoride (16.5 mg, 6.3 mmol) at room temperature. After stirring for 5 h, the resulting mixture was poured into cool water (20 mL) and extracted with EtOAc (3 × 20 mL). The combined organic layers were washed with water (50 mL), brine (50 mL), dried over anhydrous MgSO₄, filtered, and concentrated *in vacuo*. The residue was purified by chromatography on silica gel gave compound 8 as a colorless liquid (0.83 g, 92%). ¹H NMR (500 MHz, CDCl₃) δ (ppm): 7.43 (d, *J* = 10.0, 1H), 6.95 (s, 1H), 5.18–5.15 (m, 3H), 5.07 (d, *J* = 10.0 Hz, 1H), 5.02–4.92 (m, 2H), 4.83 (s, 1H), 3.63 (s, 3H), 3.46 (s, 3H), 2.10 (s, 3H), 1.68 (s, 3H), 1.51 (d, *J* = 5.0 Hz, 3H). ESI-MS *m/z*: 377.1 (M + Na)⁺.

4.1.8. Synthesis of 1-[3-acetyl-2,6-bis(methoxymethoxy)phenyl]-2-methylallyl acetate (9)

To a stirring solution of 1-[3-(1-hydroxyethyl)-2,6-bis(methoxymethoxy)phenyl]-2-methylallyl acetate (8) (0.8 g, 2.34 mmol) in dry CH₂Cl₂ (10 mL) at 0 °C was added Dess-Martin periodinane (3.0 g, 7.1 mmol) slowly. After 4 h, the mixture was taken up in saturated aqueous NaHCO₃ (10 mL) and the aqueous layer was extracted with EtOAc (3 × 10 mL). The combined organic layers were washed with water (30 mL), brine (30 mL), dried over anhydrous MgSO₄, filtered, and concentrated *in vacuo*. The residue was purified by chromatography on silica gel gave compound 9 as a colorless liquid (0.54 g, 63%). ¹H NMR (500 MHz, CDCl₃) δ (ppm): 7.55 (d, *J* = 10.0, 1H), 6.93 (d, *J* = 5.0 Hz, 1H), 6.85 (s, 1H), 5.21–5.18 (m, 2H), 5.00–4.92 (m, 3H), 4.84 (s, 1H), 3.50 (s, 3H), 3.46 (s, 3H), 2.57 (s, 3H), 2.09 (s, 3H), 1.71 (s, 3H). ESI-MS *m/z*: 375.1 (M + Na)⁺.

4.1.9. General procedure for synthesis of sanjuanolid derivatives S01-S18

To a stirring solution of 1-[3-acetyl-2,6-bis(methoxymethoxy) phenyl]-2-methylallyl acetate (9) (145 mg, 0.41 mmol) and various substituted benzaldehydes (0.41 mmol) in EtOH (8 mL), KOH (69 mg,

1.2 mmol) was added slowly. The reaction mixture was stirred at room temperature for 16 h, then quenched with saturated aqueous NH_4Cl solution (10 mL) and extracted with EtOAc (3×10 mL). The combined organic layers were concentrated under reduced pressure. The residue was then dissolved in MeOH (6 mL), followed by 4 mol/L HCl dropwise, and the reaction mixture was stirred for 1.5 h at 70 °C. The resulting mixture was quenched with saturated aqueous NH_4Cl solution (10 mL) and extracted with EtOAc (3×10 mL). The combined organic layers were washed with water (30 mL), brine (30 mL), dried over anhydrous MgSO_4 , filtered, and concentrated *in vacuo*. The residue was purified by chromatography on silica gel to give target compounds **S01–S18**.

4.1.9.1. (E)-1-[2,4-Dihydroxy-3-(1-hydroxy-2-methylallyl)phenyl]-3-phenylprop-2-en-1-one (S01). Yellow powder, 46% yield, m.p: 147.3–150.1 °C. ^1H NMR (500 MHz, CDCl_3) δ (ppm): 13.6 (s, 1H), 7.86 (d, $J = 15.0$ Hz, 1H), 7.67–7.63 (m, 4H), 7.55 (d, $J = 15.0$ Hz, 1H), 7.42–7.41 (m, 3H), 6.56 (s, 1H), 6.36 (d, $J = 5.0$ Hz, 1H), 4.80 (s, 2H), 3.58–3.56 (m, 1H), 1.81 (s, 3H). ^{13}C NMR (126 MHz, CDCl_3) δ (ppm): 192.1, 160.1, 159.3, 144.3, 134.9, 130.6, 129.8, 128.9, 128.5, 120.4, 114.5, 112.8, 110.7, 107.4, 69.7, 29.3, 18.9. ESI-MS m/z : 309.3 (M - H) $^-$.

4.1.9.2. (E)-1-(4-Bromophenyl)-1-[2,4-dihydroxy-3-(1-hydroxy-2-methylallyl)phenyl]prop-2-en-1-one (S02). Yellow powder, 43.2% yield, m.p: 195.6–198.3 °C. ^1H NMR (500 MHz, CDCl_3) δ (ppm): 13.50 (s, 1H), 7.79 (d, $J = 15.0$ Hz, 1H), 7.65 (d, $J = 9.0$ Hz, 1H), 7.56–7.49 (m, 5H), 6.56 (s, 1H), 6.37 (d, $J = 9.0$ Hz, 1H), 4.78 (s, 2H), 1.82 (s, 3H). ^{13}C NMR (126 MHz, CDCl_3) δ (ppm): 191.7, 160.1, 159.4, 142.8, 133.8, 132.2, 129.8, 128.6, 124.9, 121.0, 114.4, 112.7, 110.8, 107.5, 69.7, 28.5, 18.9. ESI-MS m/z : 387.2 (M - H) $^-$.

4.1.9.3. (E)-1-[2,4-Dihydroxy-3-(1-hydroxy-2-methylallyl)phenyl]-3-(4-nitrophenyl)prop-2-en-1-one (S03). Yellow powder, 38.4% yield, m.p: 151.3–153.7 °C. ^1H NMR (500 MHz, CDCl_3) δ (ppm): 13.69 (s, 1H), 9.25 (s, 1H), 8.29 (d, $J = 10.0$ Hz, 2H), 7.87 (d, $J = 15.0$ Hz, 1H), 7.80–7.78 (m, 3H), 7.70 (d, $J = 15.0$ Hz, 1H), 6.51 (d, $J = 5.0$ Hz, 1H), 5.92 (s, 1H), 5.16 (s, 1H), 5.00 (s, 1H), 1.82 (s, 3H). ^{13}C NMR (126 MHz, CDCl_3) δ (ppm): 191.1, 164.3, 163.6, 144.3, 141.0, 140.9, 137.2, 130.9, 128.9, 124.3, 113.2, 113.1, 112.6, 109.7, 104.3, 72.7, 18.4. ESI-MS m/z : 354.1 (M - H) $^-$.

4.1.9.4. (E)-1-[2,4-Dihydroxy-3-(1-hydroxy-2-methylallyl)phenyl]-3-[2-(trifluoromethyl)phenyl]prop-2-en-1-one (S04). Yellow powder, 35.3% yield, m.p: 123.7–126.5 °C. ^1H NMR (500 MHz, CDCl_3) δ (ppm): 13.43 (s, 1H), 7.87 (d, $J = 20.0$ Hz, 2H), 7.80 (s, 1H), 7.68 (d, $J = 20.0$ Hz, 2H), 7.59–7.54 (m, 2H), 6.57 (s, 1H), 6.39 (d, $J = 10.0$ Hz, 1H), 4.79 (s, 2H), 1.83 (s, 3H). ^{13}C NMR (126 MHz, CDCl_3) δ (ppm): 199.1, 158.8, 155.4, 146.7, 143.4, 132.1, 131.5, 130.6, 127.9, 127.4, 125.3, 110.1, 109.3, 105.3, 105.0, 101.8, 94.4, 69.9, 19.9. ESI-MS m/z : 377.1 (M - H) $^-$.

4.1.9.5. (E)-1-[2,4-Dihydroxy-3-(1-hydroxy-2-methylallyl)phenyl]-3-[3-(trifluoromethyl)phenyl]prop-2-en-1-one (S05). Yellow powder, 42.6% yield, m.p: 127.6–131.3 °C. ^1H NMR (500 MHz, CDCl_3) δ (ppm): 13.43 (s, 1H), 7.86–7.82 (m, 3H), 7.65 (d, $J = 5.0$ Hz, 1H), 7.59–7.54 (m, 3H), 6.54 (s, 1H), 6.36 (d, $J = 5.0$ Hz, 1H), 4.76 (s, 2H), 3.56 (s, 1H), 1.80 (s, 3H). ^{13}C NMR (126 MHz, CDCl_3) δ (ppm): 191.4, 160.1, 159.5, 142.2, 135.7, 131.7, 129.9, 129.5, 128.7, 126.8, 124.7, 124.6, 122.2, 114.4, 112.6, 110.7, 107.6, 107.4, 69.7, 46.4, 18.9. ESI-MS m/z : 377.1 (M - H) $^-$.

4.1.9.6. (E)-1-[2,4-Dihydroxy-3-(1-hydroxy-2-methylallyl)phenyl]-3-(4-(trifluoromethyl)phenyl)prop-2-en-1-one (S06). Yellow powder, 44.1% yield, m.p: 178.8–181.6 °C. ^1H NMR (500 MHz, CDCl_3) δ (ppm): 13.42 (s, 1H), 7.86 (d, $J = 15.0$ Hz, 1H), 7.74 (d, $J = 10.0$ Hz, 2H), 7.69–7.63 (m, 4H), 6.57 (s, 1H), 6.38 (s, 1H), 4.79 (s, 2H), 1.83 (s, 3H). ^{13}C NMR (126 MHz, CDCl_3) δ (ppm): 191.2, 160.2, 159.6, 142.1, 138.3, 136.7, 129.8, 128.5, 125.9, 125.9, 114.4, 112.7, 110.8, 107.6, 69.8, 18.9. ESI-

MS m/z : 377.1 (M - H) $^-$.

4.1.9.7. (E)-1-[2,4-Dihydroxy-3-(1-hydroxy-2-methylallyl)phenyl]-3-[4-(4-methylpiperazin-1-yl)phenyl]prop-2-en-1-one (S07). Yellow powder, 48.7% yield, m.p: 68.6–70.1 °C. ^1H NMR (500 MHz, CDCl_3) δ (ppm): 7.54–7.64 (m, 1H), 7.23 (d, $J = 8.5$ Hz, 1H), 7.14 (d, $J = 8.7$ Hz, 1H), 6.86 (dd, $J = 14.2$, 5.7 Hz, 2H), 6.53 (s, 1H), 6.32 (d, $J = 8.7$ Hz, 1H), 5.52 (s, 1H), 4.76 (s, 3H), 3.20–3.30 (m, 6H), 2.62 (dd, $J = 18.3$, 12.8 Hz, 7H), 1.83 (s, 3H). ^{13}C NMR (126 MHz, CDCl_3) δ (ppm): 190.3, 163.2, 160.1, 146.5, 145.4, 131.8, 130.5, 130.2, 127.3, 125.1, 116.0, 114.8, 113.7, 109.3, 105.1, 70.1, 54.6, 46.9, 45.9, 19.6. ESI-MS m/z : 409.0 (M + H) $^+$.

4.1.9.8. (E)-1-[2,4-Dihydroxy-3-(1-hydroxy-2-methylallyl)phenyl]-3-(4-morpholinophenyl)prop-2-en-1-one (S08). Yellow powder, 36.3% yield, m.p: 87.8–91.2 °C. ^1H NMR (500 MHz, CDCl_3) δ (ppm): 14.2 (s, 1H), 7.87 (d, $J = 15.4$ Hz, 1H), 7.84 (d, $J = 11.6$ Hz, 1H), 7.58 (d, $J = 8.6$ Hz, 1H), 7.43 (d, $J = 15.4$ Hz, 1H), 6.91 (d, $J = 8.6$ Hz, 2H), 6.73 (d, $J = 9.0$ Hz, 1H), 5.63 (s, 1H), 5.30–5.25 (m, 2H), 5.01 (s, 1H), 4.91 (s, 1H), 3.87 (s, 4H), 3.48 (s, 3H), 3.29 (s, 4H), 1.79 (s, 3H). ^{13}C NMR (500 MHz, CDCl_3) δ (ppm): 192.6, 163.3, 160.2, 152.9, 146.5, 145.3, 130.4, 125.6, 118.2, 116.3, 115.4, 114.6, 109.3, 105.1, 94.2, 77.3, 77.0, 76.8, 66.6, 56.5, 47.9, 19.6. ESI-MS m/z : 418.4 (M + Na) $^+$.

4.1.9.9. (E)-1-[2,4-Dihydroxy-3-(1-hydroxy-2-methylallyl)phenyl]-3-(2-methoxyphenyl)prop-2-en-1-one (S09). Yellow liquid, 38.2% ^1H NMR (400 MHz, CDCl_3) δ (ppm): 13.73 (s, 1H), 8.19 (d, $J = 15.6$ Hz, 1H), 7.81 (d, $J = 8.82$ Hz, 1H), 7.71 (d, $J = 15.6$ Hz, 1H), 7.63 (d, $J = 6.08$ Hz, 1H), 7.39 (t, $J = 7.48$ Hz, 1H), 7.00 (t, $J = 7.48$ Hz, 1H), 6.95 (d, $J = 8.32$ Hz, 1H), 6.54 (d, $J = 8.82$ Hz, 1H), 6.29 (s, 1H), 4.07 (s, 2H), 3.93 (s, 3H), 1.67 (s, 3H). ^{13}C NMR (101 MHz, CDCl_3) δ (ppm): 192.7, 163.8, 159.3, 158.9, 141.9, 140.1, 131.9, 130.6, 129.5, 123.8, 121.0, 120.8, 115.9, 113.9, 111.9, 111.3, 107.0, 58.3, 55.6, 15.9. ESI-MS m/z : 338.4 (M - H) $^-$.

4.1.9.10. (E)-1-[2,4-Dihydroxy-3-(1-hydroxy-2-methylallyl)phenyl]-3-(3-methoxyphenyl)prop-2-en-1-one (S10). Yellow liquid, 36.9% ^1H NMR (400 MHz, CDCl_3) δ (ppm): 13.73 (s, 1H), 7.87 (d, $J = 15.4$ Hz, 1H), 7.70 (d, $J = 8.88$ Hz, 1H), 7.63 (d, $J = 8.68$ Hz, 2H), 7.47 (d, $J = 15.4$ Hz, 1H), 6.97 (d, $J = 8.68$ Hz, 2H), 6.60 (s, 1H), 6.39 (d, $J = 8.88$ Hz, 1H), 4.80 (s, 2H), 4.11 (s, 3H), 1.85 (s, 3H). ^{13}C NMR (101 MHz, CDCl_3) δ (ppm): 192.1, 163.9, 163.3, 160.0, 144.9, 144.4, 130.5, 130.0, 121.2, 120.7, 120.4, 120.3, 116.6, 116.4, 115.8, 1137, 107.2, 103.1, 102.8, 55.4, 29.7, 16.6. ESI-MS m/z : 338.4 (M - H) $^-$.

4.1.9.11. (E)-1-[2,4-Dihydroxy-3-(1-hydroxy-2-methylallyl)phenyl]-3-(4-methoxyphenyl)prop-2-en-1-one (S11). Yellow liquid, 39.4%. ^1H NMR (400 MHz, CDCl_3) δ (ppm): 13.89 (s, 1H), 7.90 (d, $J = 15.4$ Hz, 1H), 7.85 (d, $J = 8.96$ Hz, 1H), 7.64 (d, $J = 8.56$ Hz, 2H), 7.52 (d, $J = 15.4$ Hz, 1H), 6.98 (d, $J = 8.56$ Hz, 2H), 6.58 (d, $J = 8.96$ Hz, 1H), 6.32 (s, 1H), 4.10 (s, 2H), 3.89 (s, 3H), 1.71 (s, 3H). ^{13}C NMR (101 MHz, CDCl_3) δ (ppm): 192.1, 163.8, 161.8, 159.3, 144.35, 141.9, 130.4, 127.6, 117.8, 115.9, 114.5, 113.9, 111.9, 107.1, 58.4, 55.5, 15.9. ESI-MS m/z : 338.3 (M - H) $^-$.

4.1.9.12. (E)-1-[2,4-Dihydroxy-3-(1-hydroxy-2-methylallyl)phenyl]-3-(2,3-dimethoxyphenyl)prop-2-en-1-one (S12). Yellow powder, 43.6% yield, m.p: 135.2–138.9 °C. ^1H NMR (500 MHz, CDCl_3) δ (ppm): 13.59 (s, 1H), 8.15 (d, $J = 20.0$ Hz, 1H), 7.66–7.62 (m, 2H), 7.09 (d, $J = 10.0$ Hz, 1H), 6.98 (d, $J = 5.0$ Hz, 1H), 6.57 (s, 1H), 6.35 (d, $J = 10.0$ Hz, 1H), 4.76 (s, 2H), 3.90 (s, 6H), 1.81 (s, 3H). ^{13}C NMR (126 MHz, CDCl_3) δ (ppm): 192.4, 160.1, 159.2, 153.3, 149.2, 139.2, 129.8, 129.0, 124.2, 121.9, 119.9, 114.4, 112.8, 110.7, 107.4, 69.7, 61.3, 55.9, 18.9. ESI-MS m/z : 371.2 (M + H) $^+$.

4.1.9.13. (E)-1-[2,4-Dihydroxy-3-(1-hydroxy-2-methylallyl)phenyl]-3-(3,4-dimethoxyphenyl)prop-2-en-1-one (S13). Yellow powder, 42.5%

yield, m.p: 169.3–173.6 °C. ¹H NMR (500 MHz, CDCl₃) δ (ppm): 13.68 (s, 1H), 7.83 (d, *J* = 15.0 Hz, 1H), 7.69 (d, *J* = 10.0 Hz, 1H), 7.42 (d, *J* = 15.0 Hz, 1H), 7.24 (d, *J* = 10.0 Hz, 1H), 7.15 (s, 1H), 6.90 (d, *J* = 10.0 Hz, 1H), 6.57 (s, 1H), 6.37 (d, *J* = 5.08 Hz, 1H), 4.77 (s, 2H), 3.96 (s, 3H), 3.94 (s, 3H), 1.82 (s, 3H). ¹³C NMR (126 MHz, CDCl₃) δ (ppm): 191.9, 160.1, 159.1, 151.6, 149.4, 144.4, 129.7, 128.5, 127.9, 123.3, 118.1, 114.6, 112.83, 111.2, 110.3, 107.2, 69.7, 56.0 (d), 19.0. ESI-MS *m/z*: 371.0 (M + H)⁺.

4.1.9.14. (*E*)-1-[2,4-Dihydroxy-3-(1-hydroxy-2-methylallyl)phenyl]-3-(2,4-dimethoxyphenyl) prop-2-en-1-one (S14). Yellow powder, 45.7% yield, m.p: 177.6–180.5 °C. ¹H NMR (500 MHz, CDCl₃) δ (ppm): 8.12 (d, *J* = 15.0 Hz, 1H), 7.67 (d, *J* = 8.8 Hz, 1H), 7.58 (d, *J* = 15.0 Hz, 1H), 7.57 (d, *J* = 10.0 Hz, 1H), 6.58–6.52 (m, 2H), 6.48 (s, 1H), 6.36 (d, *J* = 10.0 Hz, 1H), 4.76 (s, 2H), 3.92 (s, 3H), 3.87 (s, 3H), 1.82 (s, 3H). ¹³C NMR (126 MHz, CDCl₃) δ (ppm): 192.7, 163.6, 163.2, 160.6, 142.5, 140.0, 131.2, 130.8, 118.5, 117.2, 113.5, 113.3, 111.3, 108.6, 105.5, 98.6, 79.9, 77.3, 77.0, 76.8, 65.4, 55.6, 55.5, 18.5. ESI-MS *m/z*: 371.2 (M + H)⁺.

4.1.9.15. (*E*)-1-[2,4-Dihydroxy-3-(1-hydroxy-2-methylallyl)phenyl]-3-(2,5-dimethylphenyl) prop-2-en-1-one (S15). Yellow powder, 49.6% yield, m.p: 127.6–130.3 °C. ¹H NMR (500 MHz, CDCl₃) δ (ppm): 13.61 (s, 1H), 8.16 (d, *J* = 15.0 Hz, 1H), 7.70 (d, *J* = 10.0 Hz, 1H), 7.50–7.46 (m, 2H), 7.13 (s, 2H), 6.58 (s, 1H), 6.38 (d, *J* = 5.0 Hz, 1H), 5.35–5.30 (m, 1H), 4.78 (s, 2H), 2.45 (s, 3H), 2.37 (s, 3H), 1.83 (s, 3H). ¹³C NMR (126 MHz, CDCl₃) δ (ppm): 191.1, 159.1, 158.2, 141.1, 134.8, 134.5, 132.6, 130.3, 129.9, 128.9, 127.4, 125.9, 120.1, 113.5, 111.8, 109.7, 106.4, 68.7, 19.9, 18.3, 17.9. ESI-MS *m/z*: 338.3 (M - H)⁺.

4.1.9.16. (*E*)-1-[2,4-Dihydroxy-3-(1-hydroxy-2-methylallyl)phenyl]-3-(4-hydroxy-3-methoxy phenyl)prop-2-en-1-one (S16). Yellow powder, 32.4% yield, m.p: 143.6–147.5 °C. ¹H NMR (500 MHz, CDCl₃) δ (ppm): 14.02 (s, 1H), 7.87–7.84 (s, 2H), 7.45 (d, *J* = 15.0 Hz, 1H), 7.25–7.13 (m, 3H), 6.75 (d, *J* = 10.0 Hz, 2H), 5.64 (s, 1H), 5.50 (s, 1H), 5.28 (s, 2H), 5.01 (s, 1H), 4.92 (s, 1H), 3.94 (s, 3H), 1.79 (s, 3H). ¹³C NMR (126 MHz, CDCl₃) δ (ppm): 192.6, 163.3, 160.3, 150.3, 149.2, 146.4, 145.3, 130.4, 128.8, 122.9, 118.2, 117.0, 115.3, 112.0, 109.4, 105.2, 97.2, 94.2, 62.2, 56.6, 19.6. ESI-MS *m/z*: 357.2 (M + H)⁺.

4.1.9.17. (*E*)-1-[2,4-Dihydroxy-3-(1-hydroxy-2-methylallyl)phenyl]-3-(2,4,6-trimethoxyphenyl) prop-2-en-1-one (S17). Yellow powder, 44.2% yield, m.p: 116.4–118.3 °C. ¹H NMR (500 MHz, CDCl₃) δ (ppm): 14.04 (s, 1H), 8.32 (d, *J* = 15.0 Hz, 1H), 7.91 (d, *J* = 15.0 Hz, 1H), 7.65 (d, *J* = 5.0 Hz, 1H), 6.58 (s, 1H), 6.34 (d, *J* = 10.0 Hz, 1H), 6.13 (s, 2H), 4.75 (s, 2H), 3.92 (s, 6H), 3.86 (s, 3H), 1.81 (s, 3H). ¹³C NMR (126 MHz, CDCl₃) δ (ppm): 193.8, 163.4, 161.9 (d), 160.00, 158.5, 135.6, 129.7, 128.2, 119.8, 115.0, 113.1, 110.6, 106.9, 106.7, 90.6 (d), 69.6, 55.9 (d), 55.4, 18.9. ESI-MS *m/z*: 401.3 (M + H)⁺.

4.1.9.18. (*E*)-1-[2,4-Dihydroxy-3-(1-hydroxy-2-methylallyl)phenyl]-3-(3,4,5-trimethoxyphenyl) prop-2-en-1-one (S18). Yellow powder, 47.5% yield, m.p: 142.8–145.1 °C. ¹H NMR (500 MHz, CDCl₃) δ (ppm): 13.60 (s, 1H), 7.78 (d, *J* = 15.0 Hz, 1H), 7.67 (d, *J* = 10.0 Hz, 1H), 7.45–7.43 (m, 1H), 6.86 (s, 2H), 6.57 (s, 1H), 6.41 (d, *J* = 10.0 Hz, 1H), 4.77 (s, 2H), 3.93 (s, 6H), 3.90 (s, 3H), 1.82 (s, 3H). ¹³C NMR (126 MHz, CDCl₃) δ (ppm): 191.9, 160.1, 159.2, 153.5 (d), 144.4, 140.7, 130.3, 129.7, 128.5, 119.6, 114.5, 112.8, 110.8, 107.3, 105.9 (d), 69.7, 61.0, 56.3 (d), 18.9. ESI-MS *m/z*: 399.1 (M - H)⁺.

4.2. Cell culture

Castration-resistant Prostate Cancer (CRPC) PC3 and DU145 cells, human normal hepatic cells (MIHA) and human normal prostatic stromal myofibroblast cells (WPMY-1) were obtained from the Cell Resource

Center of Peking Union Medical College and were cultured at 37 °C under 5% CO₂ in DMEM (Dulbecco's Modified Eagle Medium) supplemented with 10% fetal calf serum (PPA) and 100 U/mL penicillin and streptomycin (HyClone™).

4.3. Cell viability assay

The cell viability was assessed with the 3-(4,5-dimethylthiazol-2-yl)-2,5-diphenyltetrazolium bromide (MTT) assay as described previously [30]. Cells (4 × 10³ cells/well in 96-well plates) were incubated at 37 °C with or without S07 treatment for 48 h, after which MTT (0.5 mg/mL) was added at 20 μL/well for another 4 h. The reaction product, formazan, was dissolved in 100 μL of DMSO after discarding the culture medium. Cell viability was determined by reading the absorbance at 560 nm by a spectrophotometer (DTX880, Beckman Coulter, CA, USA).

4.4. Long-term proliferation studies

PC3 and DU145 cells (5.0 × 10⁵) were seeded in a 10 cm² dish. After 6 h, S07 was added to a final concentration of 4.0, 8.0 or 16.0 μM. The medium was changed every three days until confluency was reached [31].

4.5. Western blot

Cells were lysed and boiled for 10 min. Proteins were separated by SDS-PAGE, transferred to a PVDF membrane and detected with relevant antibodies against cleaved-PARP (CST), caspase-3 (CST), cleaved-caspase-3 (CST), γ-H2AX (CST) or GAPDH (CST).

4.6. Cell cycle distribution analysis

Cells were cultured in the absence or presence of 0, 4.0, 8.0 or 16.0 μM of S07 for 2 days or 7 days. Cells were trypsinized, washed and stained with propidium iodide before the cell cycle distribution was assessed on a flow cytometer (BD (Becton Dickinson) FACS Calibur, BD Biosciences).

4.7. Annexin V/PI apoptosis assay

Cells were seeded in 6 cm² dishes at a density of 3.0 × 10⁵ cells per dish and incubated at 37 °C for 6 h until cells attached to the dish. S07 was added to the medium at a final concentration of 0, 4.0, 8.0 or 16.0 μM. After 48 h or 7 days, cells were harvested for Annexin V/PI apoptosis assay. The assay was performed following the protocol provided by the Annexin V/PI apoptosis Kit (Sigma). The cells were assessed on a flow cytometer (BD FACSCalibur, BD Biosciences).

4.8. Senescence-associated beta-galactosidase (SA-β gal) staining assay

A beta-galactosidase (SA-β gal) staining kit was obtained from Sigma. The assay was performed following the manufacturer's instructions. In brief, cells were washed once with PBS and fixed with stationary liquid provided in the kit at room temperature for 15 min. Next, the cells were incubated overnight at 37 °C in the dark with 1 mL of a working solution containing 0.05 mg/ml of 5-bromo-4-chloro-3-indolyl-β-D-galactopyranoside (X-gal). Subsequently, the cells were observed under a normal light microscope (Nikon, Japan).

4.9. Immunofluorescence (IF) assay of DNA damage

Immunofluorescence (IF) assays were performed as previously described [31]. Briefly, cells on a coverslip were fixed with 4% paraformaldehyde and permeabilized in 0.5% Triton X-100 (in 1 × PBS). Cells were incubated overnight at 4 °C with primary antibodies against 53BP1 (CST), washed three times and incubated with secondary

antibodies (DyLight 488-conjugated anti-mouse). The coverslip was washed with PBS about three times. The cells were washed and mounted with DAPI. Fluorescence was detected and imaged using a Nikon Ti microscope. To quantify the degree of DNA damage, > 200 cells from each group were randomly chosen from three independent experiments.

4.10. Comet assay

The comet assay was used to detect DNA damage [32,33]. Briefly, cells were mixed with 0.5% low melting temperature agarose and layered on slides pre-coated with 1.5% normal agarose. Then, slides were lysed in 2.5 M NaCl, 100 mM EDTA, 10 mM Tris (pH 8.0), 0.5% Triton X-100, 3% DMSO and 1% *N*-lauroylsarcosine. Electrophoresis in 300 mM sodium acetate, 100 mM Tris-HCl and 1% DMSO was performed. The slides were then mounted with PI solution and visualized under a fluorescence microscope (Nikon Ti microscope). Analysis was performed with CASP.

4.11. Molecular docking

The crystal structure of the B-DNA dodecamer was obtained from Protein Data Bank (PDB ID: 355D). Water molecules was manually removed by using PyMol software. The predicted binding pose of compound S07 was carried out using Autodock (version 4.2.6). Prepare_ligand4.py and prepare_receptor4.py scripts from AutoDock-Tools were used to prepare the initial files including adding hydrogen atoms and charges. Next, a grid box of 60 × 60 × 60 with a spacing of 0.40 Å enclosed the whole binding site. The Lamarckian genetic (LGA) was adopted to search for the best binding poses. The specific docking settings were as follows: trials of 100 dockings, 300 individuals per population with a crossover rate of 0.8, and the local search rate set to 0.06. Other parameters were set as default during the docking.

4.12. Statistical analysis

Results are expressed as the mean ± standard error of the mean (SD). Student's *t* test or Two-way ANOVA was employed to analyze the differences between sets of data. Statistics were performed using GraphPad Pro (GraphPad, San Diego, CA, USA). *p* values < 0.05 (*p* < 0.05) were considered significant. All experiments were repeated at least three times.

Declaration of Competing Interest

The authors declare that they have no known competing financial interests or personal relationships that could have appeared to influence the work reported in this paper.

Acknowledgements

We acknowledge the support of the National Natural Science Foundation of China (81973168, 81773579 and 21701194), Wenzhou Basic Medical and Health Technology Project (Y20180177, Y20180179 and 2014Y0056) and Wenzhou Medical University Talent Start-up Fund (QTJ17022) for the financial support. We thank LetPub (www.letpub.com) for its linguistic assistance during the preparation of this manuscript.

Appendix A. . Supplementary material

Supplementary data to this article can be found online

Appendix B. Supplementary data

Supplementary data to this article can be found online at <https://doi.org/10.1016/j.bioorg.2021.104880>.

References

- [1] S.J. Hotte, F. Saad, Current management of castrate-resistant prostate cancer, *Curr Oncol* 17 (Suppl 2) (2010) S72–79.
- [2] L.A. Torre, F. Bray, R.L. Siegel, J. Ferlay, J. Lortet-Tieulent, A. Jemal, Global cancer statistics, 2012, *CA Cancer J. Clin.* 65 (2) (2015) 87–108.
- [3] M.J. Barry, L.H. Simmons, Prevention of Prostate Cancer Morbidity and Mortality: Primary Prevention and Early Detection, *Med. Clin. North Am.* 101 (4) (2017) 787–806.
- [4] Prostate Cancer Treatment (PDQ(R)): Patient Version, in: PDQ Cancer Information Summaries, Bethesda (MD), 2002.
- [5] Prostate Cancer Treatment (PDQ(R)): Health Professional Version, in: PDQ Cancer Information Summaries, Bethesda (MD), 2002.
- [6] S.A. Thurman, N.R. Ramakrishna, T.L. DeWeese, Radiation therapy for the treatment of locally advanced and metastatic prostate cancer, *Hematol. Oncol. Clin. North Am.* 15 (2001) 423–443.
- [7] A. Dellis, F. Zagouri, M. Liontos, D. Mitropoulos, A. Bamias, A.G. Papatouris, G. Hellenic Genito-Urinary Cancer, Management of advanced prostate cancer: A systematic review of existing guidelines and recommendations, *Cancer Treat Rev.* 73 (2019) 54–61.
- [8] P. Cornford, J. Bellmunt, M. Bolla, E. Briers, M. De Santis, T. Gross, A.M. Henry, S. Joniau, T.B. Lam, M.D. Mason, H.G. van der Poel, T.H. van der Kwast, O. Rouviere, T. Wiegel, N. Mottet, EAU-ESTRO-SIOG Guidelines on Prostate Cancer Part II: Treatment of Relapsing, Metastatic, and Castration-Resistant Prostate Cancer, *Eur Urol* 71 (2017) 630–642.
- [9] L.J. Scott, Enzalutamide: A Review in Castration-Resistant Prostate Cancer, *Drugs* 78 (2018) 1913–1924.
- [10] C. Ritch, M. Cookson, Recent trends in the management of advanced prostate cancer, *F1000Res*, 7 (2018).
- [11] J.Y. Teoh, C.F. Ng, D.M. Poon, Chemohormonal therapy for metastatic hormone-sensitive prostate cancer: An Asian perspective, *Asia Pac J Clin Oncol* 14 (Suppl 5) (2018) 5–8.
- [12] O. Sartor, Advanced prostate cancer update 2018, *Asia Pac J Clin Oncol* 14 (Suppl 5) (2018) 9–12.
- [13] Liang Dong, Richard C. Zieren, Wei Xue, Theo M. de Reijke, Kenneth J. Pienta, Metastatic prostate cancer remains incurable, why? *Asian J Urol* 6 (1) (2019) 26–41.
- [14] Corena V. Shaffer, Shengxin Cai, Jiangnan Peng, Andrew J. Robles, Rachel M. Hartley, Douglas R. Powell, Lin Du, Robert H. Cichewicz, Susan L. Mooberry, Texas Native Plants Yield Compounds with Cytotoxic Activities against Prostate Cancer Cells, *J. Nat. Prod.* 79 (3) (2016) 531–540.
- [15] Bo Fang, Zhongxiang Xiao, Yinda Qiu, Sheng Shu, Xianxin Chen, Xiaojing Chen, Fei Zhuang, Yunjie Zhao, Guang Liang, Zhiguo Liu, Synthesis and Anti-inflammatory Evaluation of (R)-, (S)-, and (±)-Sanjuanolidol Isolated from *Dalea frutescens*, *J. Nat. Prod.* 82 (4) (2019) 748–755.
- [16] Zhiguo Liu, Longguang Tang, Peng Zou, Yali Zhang, Zhe Wang, Qilu Fang, Lili Jiang, Gaozhi Chen, Zheng Xu, Huajie Zhang, Guang Liang, Synthesis and biological evaluation of allylated and prenylated mono-carbonyl analogs of curcumin as anti-inflammatory agents, *Eur. J. Med. Chem.* 74 (2014) 671–682.
- [17] Jeffrey R. Jackson, Denis R. Patrick, Mohammed M. Dar, Pearl S. Huang, Targeted anti-mitotic therapies: can we improve on tubulin agents? *Nat. Rev. Cancer* 7 (2) (2007) 107–117.
- [18] C.J. Sherr, The Pezcoller lecture: cancer cell cycles revisited, *Cancer Res.* 60 (2000) 3689–3695.
- [19] A.K. Tyagi, R.P. Singh, C. Agarwal, D.C. Chan, R. Agarwal, Silibinin strongly synergizes human prostate carcinoma DU145 cells to doxorubicin-induced growth inhibition, G2-M arrest, and apoptosis, *Clin. Cancer Res.* 8 (2002) 3512–3519.
- [20] A. Hamid Boulares, Alexander G. Yakovlev, Vessela Ivanova, Bogdan A. Stoica, Geping Wang, Sudha Iyer, Mark Smulson, Role of poly(ADP-ribose) polymerase (PARP) cleavage in apoptosis. Caspase 3-resistant PARP mutant increases rates of apoptosis in transfected cells, *J. Biol. Chem.* 274 (33) (1999) 22932–22940.
- [21] S. Panneer Selvam, B. Roth, R. Nganga, J. Kim, M. Cooley, K. Helke, C. Smith, B. Ogretmen, Balance between senescence and apoptosis is regulated by telomere damage-induced association between p16 and caspase-3, *J. Biol. Chem.* 293 (2018) 9784–9800.
- [22] C. Lord, A.J.N. Ashworth, The DNA damage response and cancer therapy, *Nature* 481 (2012) 287–294.
- [23] P. Bouwman, J. Jonkers, The effects of deregulated DNA damage signalling on cancer chemotherapy response and resistance, *Nat. Rev. Cancer* 12 (2012) 587–598.
- [24] N.S. Gavande, P.S. VanderVere-Carozza, H.D. Hinshaw, S.I. Jalal, C.R. Sears, K. S. Pawelczak, J.J. Turchi, DNA repair targeted therapy: The past or future of cancer treatment? *Pharmacol. Ther.* 160 (2016) 65–83.
- [25] Qiaoyan Yang, Qian Zhu, Xiaopeng Lu, Yipeng Du, Linlin Cao, Changchun Shen, Tianyun Hou, Meiting Li, Zhiming Li, Chaohua Liu, Di Wu, Xingzhi Xu, Lina Wang, Haiying Wang, Ying Zhao, Yang Yang, Wei-Guo Zhu, G9a coordinates with the RPA complex to promote DNA damage repair and cell survival, *PNAS* 114 (30) (2017) E6054–E6063.
- [26] D. Cahill, B. Connor, J.P. Carney, Mechanisms of eukaryotic DNA double strand break repair, *Front Biosci* 11 (2006) 1958–1976.
- [27] D.H. Lee, S.S. Acharya, M. Kwon, P. Drane, Y. Guan, G. Adelman, P. Kalev, J. Shah, D. Pellman, J.A. Marto, D. Chowdhury, Dephosphorylation enables the recruitment of 53BP1 to double-strand DNA breaks, *Mol. Cell* 54 (2014) 512–525.
- [28] K.J.F.O. Gurova, New hopes from old drugs: revisiting DNA-binding small molecules as anticancer agents, *Future Oncol.* 5 (2009) 1685–1704.

- [29] Y. Kholod, E. Hoag, K. Muratore, D.J.J.o.C.E. Kosenkov, Computer-Aided Drug Discovery: Molecular Docking of Diminazene Ligands to DNA Minor Groove, *J Chem Educ*, 98(2018) 882-887.
- [30] X.H. Zheng, Y.F. Zhong, C.P. Tan, L.N. Ji, Z.W. Mao, Pt(II) squares as selective and effective human telomeric G-quadruplex binders and potential cancer therapeutics, *Dalton Trans.* 41 (2012) 11807–11812.
- [31] X. Zheng, X. Nie, Y. Fang, Z. Zhang, Y. Xiao, Z. Mao, H. Liu, J. Ren, F. Wang, L. Xia, J. Huang, Y.J.J.o.t.N.C.I. Zhao, A Cisplatin Derivative Tetra-Pt(bpy) as an Oncotherapeutic Agent for Targeting ALT Cancer, *J Natl Cancer Inst*, 109 (2017).
- [32] Narendra P. Singh, The comet assay: Reflections on its development, evolution and applications, *Mutat. Res. Rev. Mutat. Res.* 767 (2016) 23–30.
- [33] P.L. Olive, J.P. Banath, The comet assay: a method to measure DNA damage in individual cells, *Nat. Protoc.* 1 (2006) 23–29.